

Wave nature of Rosensweig instability

Liu Li(李柳), Decai Li(李德才), Zhiqiang Qi(戚志强), Lu Wang(王璐), and Zhili Zhang(张志力)

Citation: Chin. Phys. B, 2024, 33 (**3**): 034701. DOI: 10.1088/1674-1056/ad1485
Journal homepage: http://cpb.iphy.ac.cn; http://iopscience.iop.org/cpb

What follows is a list of articles you may be interested in

Rayleigh-Taylor instability of viscoelastic self-rewetting film flowing down a temperature-controlled inclined substrate

Siyi An(安思亦) and Yongjun Jian(菅永军)
Chin. Phys. B, 2023, 32 (**6**): 064701. DOI: 10.1088/1674-1056/acc78b

A simplified approximate analytical model for Rayleigh-Taylor instability in elastic-plastic solid and viscous fluid with thicknesses

Xi Wang(王曦), Xiao-Mian Hu(胡晓棉), Sheng-Tao Wang(王升涛), and Hao Pan(潘昊)
Chin. Phys. B, 2021, 30 (**4**): 044702. DOI: 10.1088/1674-1056/abcf44

Segregation behavior of magnetic ions in continuous flowing solution under gradient magnetic field

Bing Ji(冀冰), Ping Wu(吴平), Han Ren(任菡), Shiping Zhang(张师平), Abdul Rehman, Li Wang(王立)
Chin. Phys. B, 2016, 25 (**7**): 074704. DOI: 10.1088/1674-1056/25/7/074704

Ferrofluid nucleus phase transitions in an external uniform magnetic field

B. M. Tanygin, S. I. Shulyma, V. F. Kovalenko, M. V. Petrychuk
Chin. Phys. B, 2015, 24 (**10**): 104702. DOI: 10.1088/1674-1056/24/10/104702

Electric field distribution around the chain of composite nanoparticles in ferrofluids

Fan Chun-Zhen (范春珍), Wang Jun-Qiao (王俊俏), Cheng Yong-Guang (程永光), Ding Pei (丁佩), Liang Er-Jun (梁二军), Huang Ji-Ping (黄吉平)
Chin. Phys. B, 2013, 22 (**8**): 084703. DOI: 10.1088/1674-1056/22/8/084703

Wave nature of Rosensweig instability

Liu Li(李柳)[1,2], Decai Li(李德才)[1,3,†], Zhiqiang Qi(戚志强)[1,2], Lu Wang(王璐)[1,2], and Zhili Zhang(张志力)[1,2]

[1] *School of Mechanical, Electronic, and Control Engineering, Beijing Jiaotong University, Beijing* 100044, *China*
[2] *Beijing Key Laboratory of Flow and Heat Transfer of Phase Changing in Micro and Small Scale, Beijing* 100044, *China*
[3] *State Key Laboratory of Tribology, Tsinghua University, Beijing* 100084, *China*

(Received 31 October 2023; revised manuscript received 30 November 2023; accepted manuscript online 12 December 2023)

The explicit analytical solution of Rosensweig instability spikes' shapes obtained by Navier–Stokes (NS) equation in diverse magnetic field H vertical to the flat free surface of ferrofluids are systematically studied experimentally and theoretically. After carefully analyzing and solving the NS equation in elliptic form, the force balanced surface equations of spikes in Rosensweig instability are expressed as cosine wave in perturbated magnetic field and hyperbolic tangent in large magnetic field, whose results both reveal the wave-like nature of Rosensweig instability. The results of hyperbolic tangent form are perfectly fitted to the experimental results in this paper, which indicates that the analytical solution is basically correct. Using the forementioned theoretical results, the total energy of the spike distribution pattern is calculated. By analyzing the energy components under different magnetic field intensities H, the hexagon–square transition of Rosensweig instability is systematically discussed and explained in an explicit way.

Keywords: ferrofluids, Rosensweig instability, hexagon–square transition

PACS: 47.65.Cb, 47.20.Ma, 47.10.ad **DOI:** 10.1088/1674-1056/ad1485

1. Introduction

Ferrofluid is a novel stable colloidal solution composed of nano-magnetic particles and non-magnetic carrier liquids. The standard Rosensweig instability of ferrofluids is the pattern of spikes emerging on the flat surface of ferrofluids under the vertical external magnetic field H with the field intensity greater than the critical field B_c.[1–4] There is a minimum requirement for magnetization M_c under the field of B_c for the spikes' activation based on the theory of Rosensweig's linear stability analysis

$$M_c^2 = \frac{2}{\mu_0}\left(1+\frac{1}{r_0}\right)\sqrt{\rho g \sigma}, \tag{1}$$

$$r_0 = \frac{\sqrt{\mu_c \mu_t}}{\mu_0}, \quad \mu_c = \frac{B}{H}, \quad \mu_t = \frac{\partial B}{\partial H}, \tag{2}$$

where the constant σ and ρ are the surface tension and density of ferrofluids, respectively. The parameter g is gravitational acceleration constant. The constants r_0, μ_c, and μ_t are relative permeabilities calculated by magnetic field intensity H and magnetic flux density B.

According to the superposition principle of magnetic field, the critical magnetic flux density B_c can be calculated as follows:

$$\boldsymbol{B}_c = \mu_0 (\boldsymbol{H}_c + \boldsymbol{M}_c). \tag{3}$$

It is worth mentioning that the linear stability analysis requires that the small perturbation of the magnetic field H_c casted on the steady flat ferrofluids surface. The small perturbation demonstrates a conclusion that the instability is correlated with the wave number $k_c = \sqrt{\rho g/\sigma}$.[5] Therefore, the corresponding wavelength $\lambda_c = 2\pi/k_c$ is introduced to illustrate the periodic distance between adjacent spikes. There is a mysterious paradox for us that the consecutive vertical external field establish discontinuous periodic peaks. The wave-like nature of Rosensweig instability is persistently unexplained systematically by linear stability analysis theory.

Another interesting phenomenon is that the pattern of spikes in Rosensweig instability exhibits unique hexagonal and square patterns.[5,6] The transition of hexagon–square pattern was firstly predicted by Gailitis in 1977.[2] The possible explanation of the construction of hexagon pattern under a low field intensity is the theory of "active ring" raised by Cao.[3] The transition from hexagon to square under a large field intensity could be attributed to the magnetic flux pinning effect proposed by Kubstrup.[7] This kind of transition is thought to be controlled by energy. Nonetheless, the nature of this transition is still unclear.

In this study, the key evidence of wave-like nature of spikes are searched carefully. The control equation of Rosensweig instability is established as well as the possible solution of such an equation is raised. Regarding the theory in this research, the wave-like nature of spikes in ferrofluids is systematically discussed. The final special spikes in external magnetic field with weak field intensity are determined as cosine wave, which is corresponded to the results of linear stability analysis theory raised by Rosensweig.[1] In con-

†Corresponding author. E-mail: lidecai@tsinghua.edu.cn

© 2024 Chinese Physical Society and IOP Publishing Ltd

trast, the form of spikes tends to be hyperbolic tangent form, which is perfectly fitted to these uniform experimental results. Based on the theoretical results, the hexagon–square transition phenomenon of Rosensweig instability is systematically discussed, which is explained by the theoretical analysis of total energy.

2. Results and discussion

2.1. Fundamental control equation of Rosensweig instability

Ferrofluids are colloidal systems, which could be regarded as a kind of uniform liquid system. Therefore, the Navier–Stokes (NS) equation is a prior equation governing the balance of body force and the movements of liquid. In additional to viscous force and gravity, the magnetic force part should be taken into consideration. It is assumed that all the changing of ferrofluids in magnetic fields are quite slow and reversible. Therefore, this "quasi-static" approximation gives a conclusion that the velocity of liquid is able to be neglected ($\boldsymbol{u} \approx 0$).[8,9] The incompressible NS equation with viscosity η can be expressed as

$$\rho \frac{\partial \boldsymbol{u}}{\partial t} = -\rho (\boldsymbol{u} \cdot \nabla) \boldsymbol{u} - \nabla p + \eta \nabla^2 \boldsymbol{u} + \boldsymbol{f_b}, \tag{4}$$

$$\nabla \cdot \boldsymbol{u} = 0. \tag{5}$$

Considering the magnetic part, the body forces can be expressed as

$$\boldsymbol{f}_\mathrm{b} = -\rho g \boldsymbol{e}_z + \mu_0 M \nabla H - \mu_0 \nabla \int_0^H M \mathrm{d}h. \tag{6}$$

The $\mu_0 M \nabla H$ part is the Kelvin force resulted from the changing field. The $\mu_0 \nabla \int_0^H M \mathrm{d}h$ part is the magnetic pressure originated from the established magnetic field.

The pressure gradient part ∇p is calculated by Young–Laplace equation[3,8]

$$p - p_\mathrm{r} = \sigma \cdot \kappa, \tag{7}$$

where the surface parameter κ (sum of the principal curvatures) can be written as

$$\kappa = -\nabla \cdot \left(\frac{\nabla z}{\sqrt{1 + (\nabla z)^2}} \right). \tag{8}$$

The parameter is defined as a single value of altitude $z = z_0(x, y)$.

After inducing the Young–Laplace equation into the NS equation, the synthetic NS equation of ferrofluids is

$$\sigma \cdot \kappa + \rho g z + p_\mathrm{r} = \mu_0 \int_0^H M \mathrm{d}h + \frac{1}{2} \mu_0 M_n^2, \tag{9}$$

where M_n is defined as the magnetization perpendicular to the ferrofluids surface, which contributes to the magnetic pressure jump of ferrofluids' surface.

2.2. Experimental equipment

The stable ferrofluids with explicit physical–chemical properties were obtained from the prior work.[10–12] As shown in Fig. 1, the ferrofluids are placed into a uniform magnetic field to observe the Rosensweig instability. For the purpose of ensuring the magnetic field to be a uniform field, the large coils with iron core and currents with strong field intensity are established. The area of uniform field is as large as a circular region with a diameter of 5 cm. The field intensity of magnetic fields could be controlled by the currents in coils. The voltage and currents could be controlled by 2 external DC power supplies. The platform is kept parallel to the sea level to ensure that gravity is parallel to the magnetic field.

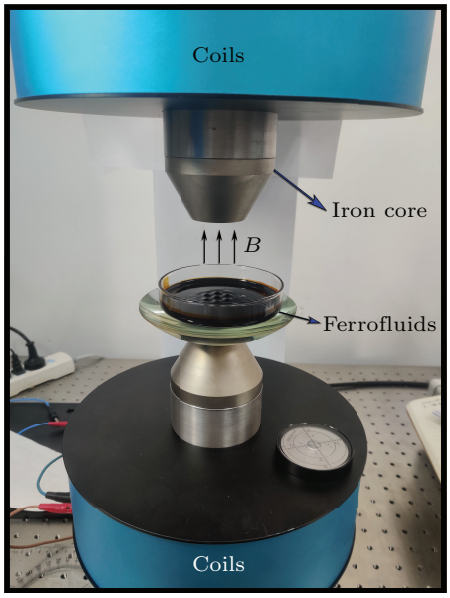


Fig. 1. Ferrofluids in vertical uniform magnetic field established by 2 coils.

2.3. Boundary shaping and potential well model

As depicted in Fig. 2, the Rosensweig instability of engine oil based ferrofluids within square-shaped boundary condition is observed. When the field intensity is lower than 12.7 mT, the spikes are not able to be established. If the field intensity is increased to larger than 12.7 mT, the spikes show up. This phenomenon proves that there is a critical field B_c, which could be the threshold field intensity of Rosensweig instability. Another result is that the peak distribution is regular hexagon. As the external field increases to 13.5 mT, a larger hexagon distribution of spikes composed of the former hexagon and other 12 spikes are constructed. When the field intensity increases to 15.5 mT, the spikes' distribution presents a standard square shape. This is evidence of the hexagon–square transformation phenomenon. However, the Rosensweig instability in a square-shaped container could not provide the evidence of wave-like nature of Rosensweig instability in ferrofluids. In this study, one of target is to explain

the hexagon–square transformation phenomenon through energy ways.

To convince the researchers of the wave-like nature of Rosensweig instability in this study, the square-shaped container is replaced by the triangle shaped container. When the magnetic field intensity is increased to a certain valve, the spikes distribution could follow the shape of container. As shown in Fig. 3, the distribution of spikes follows the shape of the container (a triangular distribution). In contrast, the spikes follow a square distribution in a square container in Figs. 2(c) and 2(d). Due to this "boundary shaping effects", the distribution patterns of spikes could be controlled by the existence of boundary. It is concluded that the Rosensweig instability could have wave's properties (wave could shaped by boundary conditions), which is highly consistent with the finite square well model in quantum physics explained by Schrödinger equation.[13] The resultant wave patterns are controlled by the boundary condition in potential well, which is highly corresponded with experimental result in this study. There must be a wave explanation of spikes' distribution and existence. Therefore, the focus is casted on the NS equation of the results.

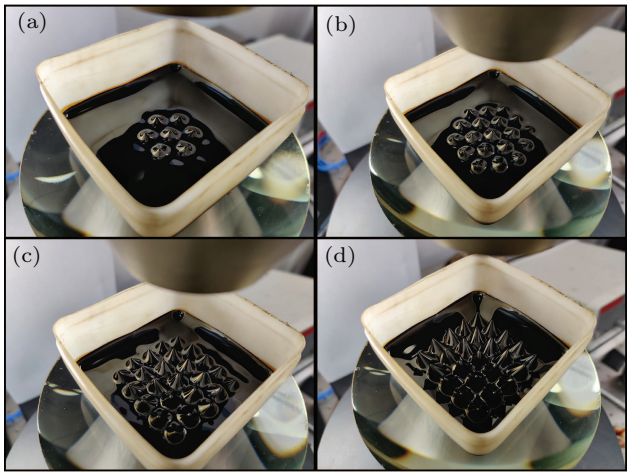


Fig. 2. Rosensweig instability of engine oil-based ferrofluids within square-shaped boundary condition. Magnetic fields' strength: (a) 12.7 mT, (b) 13.5 mT, (c) 15.5 mT, (d) 22.0 mT.

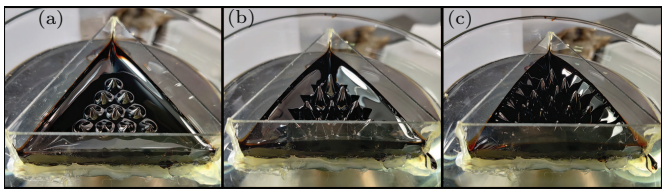


Fig. 3. Rosensweig instability of engine oil-based ferrofluids within triangle shaped boundary condition. Magnetic fields' strength: (a) 14.5 mT, (b) 47.0 mT, (c) 69.0 mT.

2.4. Elliptical wave equation of ferrofluids

The NS equation in ferrofluids is presented as Eq. (9). Here comes a definition of average magnetization:[1]

$$\bar{M} = \frac{\int_0^H M\,\mathrm{d}h}{\int_0^H \mathrm{d}h}. \tag{10}$$

Therefore, the interfacial pressure balance equation of ferrofluids can be written as

$$\sigma \cdot \kappa + \rho g z + p_{\mathrm{r}} - \mu_0 \bar{M} H - \frac{1}{2}\mu_0 M_n^2 = 0. \tag{11}$$

Afterwards, the surface parament κ in Eq. (8) are induced, and the NS equation can be further manipulated as

$$\sigma\left(\frac{\partial^2 z}{\partial x^2} + \frac{\partial^2 z}{\partial y^2}\right) + \left(\rho g z + p_{\mathrm{r}} - \mu_0 \bar{M} H - \frac{1}{2}\mu_0 M_n^2\right) \times \sqrt{1 + \left(\frac{\partial z}{\partial x}\right)^2 + \left(\frac{\partial z}{\partial y}\right)^2} = 0. \tag{12}$$

This equation is an elliptical partial differential equation, which contains the wave properties of Rosensweig instability that is simply constructed by continuous magnetic field and stable ferrofluids. However, it is difficult to address the issue of such a second order partial differential equation without any assumption. The results of this NS equation are largely infected by the boundary conditions. As shown in Figs. 2 and 3, the infinite plane model (low magnetic field intensity), the finite square well and the finite triangular well present different types of experimental results. It is important to define the boundary condition to obtain a certain solution of this static ferrofluids NS equation. Notably, the gravity and magnetism are both forces with intrinsic energy, which could be regarded as gravitational potential and magnetic energy.

Herein, the gravity and external pressure can be defined as the potential of force casted on the ferrofluids

$$V(x,y) = \rho g z(x,y) + p_{\mathrm{r}}. \tag{13}$$

Another definition of energy of magnetic field and magnetic forces can be defined as

$$E_{\mathrm{m}}(x,y) = \mu_0 \bar{M} H + \frac{1}{2}\mu_0 M_n^2. \tag{14}$$

The NS equation of ferrofluids in static magnetic field can further be written as

$$\sigma \nabla^2 z + (V - E_{\mathrm{m}}) \cdot \sqrt{1 + (\nabla z)^2} = 0. \tag{15}$$

The equation consists of elliptic wave part $\sigma\nabla^2 z$ and energy term of $(V - E_{\mathrm{m}}) \cdot \sqrt{1 + (\nabla z)^2}$. These two parts reveal some kinds of "wave–particle dualism" in Rosensweig instability of ferrofluids under the norm static magnetic field.

2.5. Perturbation of magnetic field in Rosensweig instability

To solve the NS equation of Rosensweig instability under weak magnetic field, the perturbation of the field is assumed. There is a relationship that valid permanently

$$1 \le \sqrt{1 + (\nabla z)^2} \le |\nabla z| + 1. \tag{16}$$

If the critical condition is put into consideration, a small perturbation could result in the tiny wave of Rosensweig instability. As shown in Fig. 4, the perturbation of "tiny wave" only appears under the external magnetic field intensity slightly larger than the critical field strength H_c. In this case, the height variation of spikes could be very small, which leads to an estimation based on Eq. (16)

$$\sqrt{1+(\nabla z)^2} \approx 1. \tag{17}$$

Herein, the NS equation of ferrofluids in static magnetic field (Eq. (15)) can be deduced as follows:

$$\sigma\nabla^2 z + \rho g z - E_m + p_r = 0. \tag{18}$$

Considering the one-dimensional (1D) situation, the variant z can be defined as a function $F(x)$ determined by a univariant x

$$z = F(x). \tag{19}$$

Therefore, $F(x)$ satisfies the equation

$$A \cdot F''(x) + B \cdot F(x) + C = 0, \tag{20}$$

where $A = \sigma$, $B = \rho g$, and $C = -E_m + p_r$. Theoretically, the C could be regarded as constant when the external magnetic field could be regarded as approximately H_c critical state. For positive A and B, this second-order ordinary differential equation (ODE) has a general solution form

$$F(x) = D_1 e^{ax} + D_2 e^{-bx} + D_3, \tag{21}$$

where D_1, D_2, D_3, a, and b could be constant. Then we have

$$\left[D_1\left(A\cdot a^2 + B\right) \;\; D_2\left(A\cdot b^2 + B\right) \;\; B + \frac{C}{D_3} \right] \begin{bmatrix} e^{ax} \\ e^{-bx} \\ D_3 \end{bmatrix} = 0. \tag{22}$$

This NS equation is validated in any situations with any variant x. Herein, this result is deduced as

$$\left[a \;\; b \;\; D_3 \right] = \left[\sqrt{-\frac{B}{A}} \;\; \sqrt{-\frac{B}{A}} \;\; -\frac{C}{B} \right]. \tag{23}$$

Parameters D_1 and D_2 are determined by the boundary conditions. If the axis is placed at the center of spikes' patterns, the solution of spikes form $F(x)$ is an even function according to the experimental results in Fig. 2. Then $D_1 = D_2$ can be obtained.

The general solution can be in the form of

$$\begin{aligned} F(x) &= D_1 \cdot \cosh(ax) + D_3 \\ &= D_1 \cos\left(\sqrt{\frac{\rho g}{\sigma}} x\right) + \frac{E_m - p_r}{\rho g}. \end{aligned} \tag{24}$$

The results depicting the 1D wave function $F(x)$ in perturbation situation is a kind of cosine wave with a wave vector k of $k_c = \sqrt{\rho g/\sigma}$, which is corresponded with the linear stability analysis theory.[5,14–17]

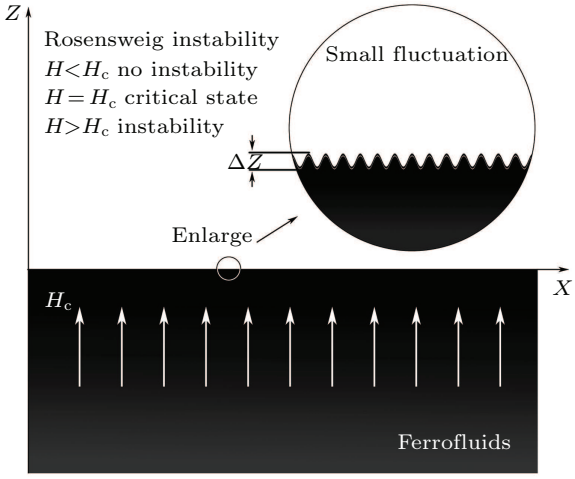


Fig. 4. Perturbation of outer field in Rosensweig instability.

2.6. Rosensweig instability with large magnetic field

The perturbation condition of external magnetic field $H = H_c + H_{perturbation}$ reveals the wave-like nature of Rosensweig instability. However, the linear stability analysis theory could only predict the Rosensweig instability when the external magnetic field is not far greater than the critical field intensity H_c. According to the experimental results in Figs. 2 and 3, the critical field intensity is 12 mT–14 mT, which is fitted to the results of other researchers.[3,5] If the field intensity increases above 20 mT, the perturbation model in linear stability analysis theory is no longer applicable. It is necessary to establish a new model to illustrate the Rosensweig instability accurately in strong magnetic field.

According to Fig. 5, the spikes could become very sharp (∇Z could be very large) due to the increment of external field. In this scenario, the new estimation based on Eq. (16) can be

$$\sqrt{1+(\nabla z)^2} \approx |\nabla z|. \tag{25}$$

Hence, the NS equation of ferrofluids in static magnetic field (Eq. (15) can be deduced as follows:

$$\sigma\nabla^2 z + (\rho g z + p_r - E_m)\cdot|\nabla z| = 0. \tag{26}$$

It is difficult to solve this partial differential equation (PDE) directly. Instead, if the 1D condition simply is put into consideration, the only variant x can determine the value of z

$$z = F(x). \tag{27}$$

Then

$$A \cdot F''(x) + B \cdot F(x) \cdot F'(x) + C \cdot F'(x) = 0, \tag{28}$$

where $A = \sigma$, $B = \rho g$, and $C = -E_m + p_r$.

For positive A and B, this second-order ordinary differential equation (ODE) processes a general solution form

$$F(x) = C_1 \cdot \sqrt{\frac{A}{B}} \tanh\left(\frac{C_1}{\sqrt{2}} \cdot \sqrt{\frac{B}{A}}(x + C_2)\right) - \frac{C}{B}. \tag{29}$$

According to this result, the constants C_1 and C_2 are determined by different boundary conditions. Here is an interesting result that the wave vector k of $k_c = \sqrt{\rho g/\sigma}$ is multiplied by a constant $C_1/\sqrt{2}$. It indicates that the wave-like nature of Rosensweig instability is influenced by boundary conditions, which is observed by the experiments in Figs. 2 and 3. The boundary condition can be very explicit that:

(i) Function $F(x)$ can be defined as an even function.

(ii) The boundary condition is a kind of periodic boundary condition.

(iii) The periodic boundary positions ought to be the peaks or valleys of spike (the maximum or minimum value of $F(x)$).

Based on the boundary conditions, the equation (29) can be deduced as

$$F(x) = C_1 \cdot \sqrt{\frac{\sigma}{\rho g}} \tanh\left(\frac{C_1}{\sqrt{2}} \cdot \sqrt{\frac{\rho g}{\sigma}} (|x| + n\lambda)\right) + \frac{E_m - p_r}{\rho g}, \tag{30}$$

where $|x|$ is the absolute value of x, n is an arbitrary integer ($n \in Z$), and λ is the wave length of Rosensweig instability.

Taking the two-dimensional (2D) conditions into consideration, the new wave function of Rosensweig instability is presented as

$$F(x) = C_1 \cdot \sqrt{\frac{\sigma}{\rho g}} \tanh\left(\frac{C_1}{\sqrt{2}} \cdot \sqrt{\frac{\rho g}{\sigma}} \left(\sqrt{x^2 + y^2} + n\lambda\right)\right) + \frac{E_m - p_r}{\rho g}. \tag{31}$$

To verify the validation of Eq. (31), the special Rosensweig instability spikes patterns under large-field intensity are observed and compared with the computational results obtained from the theoretical results. The density ρ of ferrofluids in this work is 1.346 g/cm^3, the surface tension σ of ferrofluids is 30.6 mN/m, the acceleration of gravity g is 9.8 m/s^2 and the saturated magnetization M_s of ferrofluids is 24.5 emu/g. As presented in Fig. 6, the experimental results under norm magnetic field are carefully studied. As can be seen from Figs. 2 and 3, the critical field H_c of our ferrofluids is approximately 12 mT–14 mT from results. Therefore, the applied magnetic fields strengths in these experiments are increased to be greatly larger than critical field H_c. For a certain kind of ferrofluids, the density ρ and surface tension σ are regarded as constants. It is generally believed that the magnetization of a certain kind of ferrofluids (saturated magnetization M_s is a constant) satisfied the Langevin magnetization, indicating that the magnetization only relies on the external magnetic field ($M = M(H)$) when the temperature does not varied.[3,18] In this case, the magnetic energy E_m only depends on the external field H.

From the experimental results, there are 3 kinds of spikes phenomenon in this study. Figure 6(a) exhibits a kind of symmetric spikes upside and down. The central spikes exhibit symmetric sharp spikes on the top of the roof and the down floor. Firstly, it is supposed that the $n\lambda$ of central spikes position is 0. The side spikes next to the central spikes could have a negative or positive value, $n\lambda$ ($n \in Z$). If the magnetic field intensity is not large enough, the magnetic energy E_m is less than the external pressure p_r ($E_m < p_r$). In this case, the separation of central spikes occurs. There is another special condition that the magnetic energy E_m is equal to external pressure p_r ($E_m = p_r$). The opposite central double spike can be connected through a single point, which can be seen from Fig. 6(b). If the magnetic energy E_m is larger than outer pressure p_r ($E_m > p_r$), the opposite central double spikes can be melted with each other as figure 6(c) depicted. The equation obtained is perfectly fitted to this forementioned experimental results.

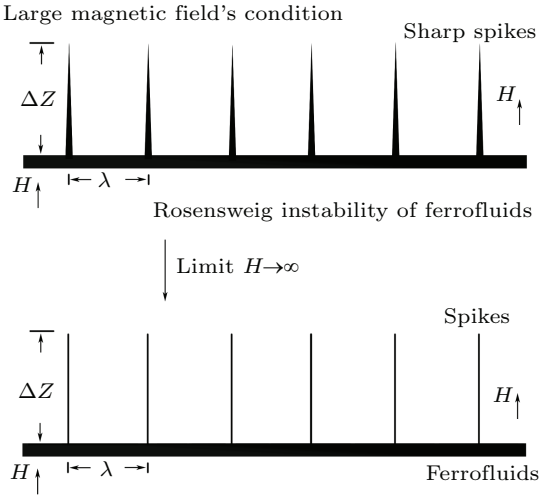


Fig. 5. Rosensweig instability with large magnetic field condition.

Considering the wavelength part $n\lambda$ in Eq. (31), there is an interesting result. If the n is enlarged from 0 to 1, the side spikes show up around the central main spike, as presented in Figs. 7(a) and 7(b). It can be seen from results that the amplitude A of side spikes is smaller than that of central spikes' amplitude. This shrinkage of amplitude of side spikes is induced by the fading magnetic field intensity from the central spikes to margin spikes (the central magnetic field intensity is larger than the margin magnetic field intensity). As depicted in Fig. 7(c), the side spikes generated by the parallel magnetic field between 2 central iron cores have an amplitude shrinkage effect. From the results obtained from Figs. 6 and 7, it can be concluded that the amplitude of spikes is controlled by external magnetic field energy E_m and the position of wave length $n\lambda$. There is a prerequisite that the magnetic field intensity decreases from central position to margin. If the field intensity is even from the center to the edge, each spike can be "central spikes". The amplitudes of spikes in this even field intensity are equal to that of the amplitude of central spikes.

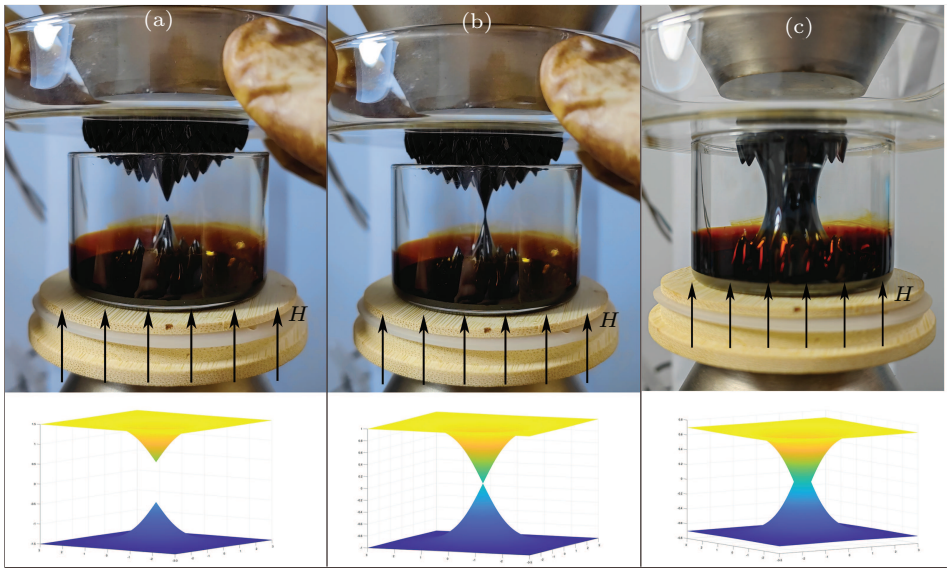


Fig. 6. Central spikes of Rosensweig instability with norm large magnetic fields: (a) symmetric spikes upside and down, ($E_m < p_r$); (b) funnel-shaped spikes connected by 1 point, ($E_m = p_r$); (c) funnel-shaped spikes partially fused, ($E_m > p_r$). Up: experimental results. Down: Computational results.

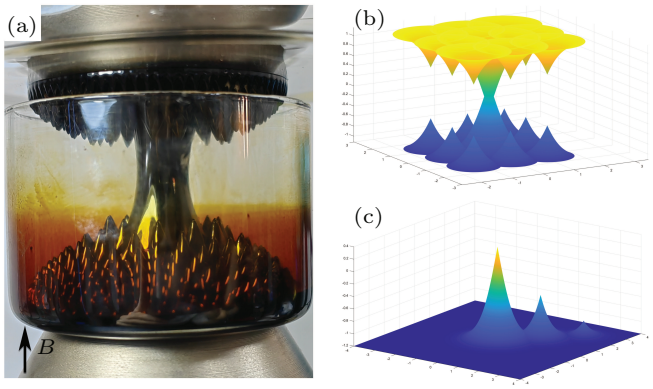


Fig. 7. Central spikes and side spikes in Rosensweig instability with norm large magnetic field condition: (a) experimental results, (b) central peaks and satellite spikes, (c) spikes with different $n\lambda$.

2.7. Energy stability of hexagon–square pattern transition in Rosensweig instability

Before considering the factors that determine the spikes' distribution patterns, it is important to determine the energy part that forms the spikes. Part of energy is the potential of repulsive magnetic forces of spikes. As shown in Fig. 8(a), it is reasonable to regard a single spike as a single magnetic momentum. The potential of repulsive forces between 2 spikes is defined as[19–21]

$$\begin{aligned} E_r &= -\frac{\mu_0}{4\pi}\left(\frac{\boldsymbol{m}_1\cdot\boldsymbol{m}_2}{r^3} - 3\frac{(\boldsymbol{m}_1\cdot r)\cdot(\boldsymbol{m}_2\cdot r)}{r^5}\right) \\ &= -\frac{\mu_0 m_1 m_2}{4\pi\cdot r^3}. \end{aligned} \tag{32}$$

As presented in Figs. 8(b) and 8(c), the spike distribution of hexagon pattern and square pattern follow a fixed pattern. It is believed that the repulsive potential decreases along with the distance of the third power ($E_r \propto 1/r^3$). Herein, the spikes are regarded as on the concentric circles centered on a central spike. The spikes on the same circle have the same distance r between themselves and central spike. This study could introduce a constant as coefficient to this infinite series, which could have a similar form as Madelung constant.[22] Therefore, the magnetic repulsive potential can be added on same circle and evaluate it by several constants β_n

$$\begin{aligned} E_r &= -\sum\frac{\mu_0 m_1 m_2}{4\pi\cdot r^3} = -\left(\sum_{n=1}^{\infty}\beta_n\right)\cdot\frac{\mu_0 m_1 m_2}{4\pi\cdot\lambda^3} \\ &= -\left(\sum_{n=1}^{\infty}\beta_n\right)\cdot\frac{\mu_0 M_s^2 V^2}{4\pi\cdot\lambda^3}, \end{aligned} \tag{33}$$

where V is the volume of a single spike. The M_s is the saturated magnetization of ferrofluids. The wavelength λ can be calculated by the equation results. The constant β_n of different patterns is presented in Table 1. It is believed that the constant β_n decreases with increasing distance. It is enough to evaluate the 6 circles close to the central spikes to estimate the infinite series of the summarization of β_n $\left(\beta_{sum} = \sum_{n=1}^{\infty}\beta_n \approx \sum_{n=1}^{6}\beta_n\right)$.

Table 1. The magnetic repulsive potential constant β_n.

	β_1	β_2	β_3	β_4	β_5	β_6	β_{sum}
Hexagon	6	1.155	0.75	0.433	0.222	0.144	8.703
Square	4	1.414	1	0.716	0.354	0.148	7.631

Except for magnetic repulsive potential E_r, the formation of magnetic spikes E_f and formation of external magnetic field E_h are essential parts of energy:

$$E_h + E_f = \iiint HB\,\mathrm{d}v = \mu_0 H(H+M_s)V. \tag{34}$$

The formation of external field ($E_h = \mu_0 H^2 V$) and the formation of magnetic spikes ($E_f = \mu_0 H M_s V$) are both infected by the external magnetic H and the volume of the single spike

V. When considering the occupied and unoccupied areas of spikes in Figs. 8(b)–8(d), the formation part of energy should be multiplied with the area utilization ratio R_a to evaluate the energy density per unit area. For hexagon patterns and square patterns, the area utilization ratios R_a are $\pi/2\sqrt{3}$ and $\pi/4$, respectively.

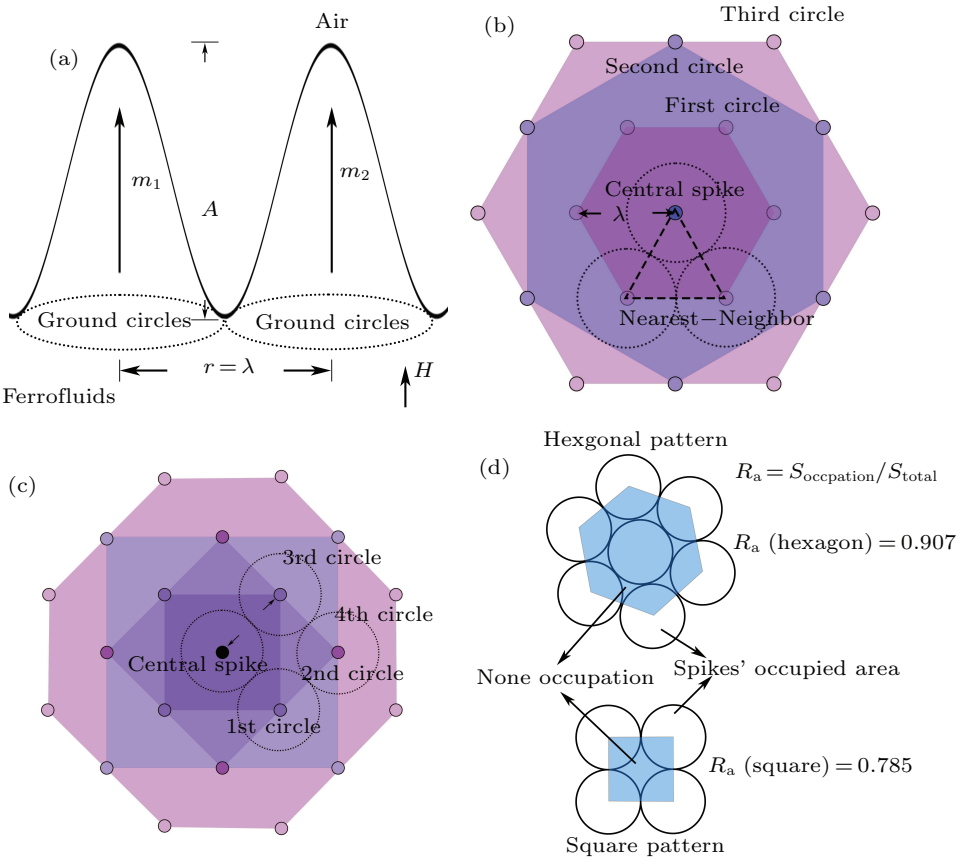


Fig. 8. (a) Magnetization and repelling forces of neighbor spikes, (b) hexagonal distribution of spikes around central spikes, (c) square distribution of spikes around central spikes, (d) the area utilization ratio R_a.

The equation of spike surface is presented in Eq. (24). The amplitude A of a single spike could be defined as[3,8,23]

$$A = e \cdot \frac{b(1+\varepsilon) + \sqrt{b^2(1+\varepsilon)^2 + 4a\varepsilon}}{2a}, \tag{35}$$

$$\varepsilon = \frac{B^2 - B_c^2}{B_c^2} \approx \frac{H^2 - H_c^2}{H_c^2}. \tag{36}$$

Based on these studies, the constants a, b, and e are defined as $a = 0.00265$, $b = 0.00293$, and $e = 3.15 \times 10^{-4}$,[3,8,23] respectively. According to the experimental results, the critical magnetic induction B_c is defined as 13 mT. The relative permeability μ_r of ferrofluids is persistently estimated as 1 ($1 < \mu_r < 1.05$). Therefore, the magnetic field is limited by the magnetization of ferrofluids. The approximation in Eq. (36) frequently applies. The total energy E_{tot} is the sum of magnetic repulsive energy E_r and formation energy of spikes E_f and external fields E_h is

$$E_{tot} = -\beta_{sum} \cdot \frac{\mu_0 M_s^2 V^2}{4\pi \cdot \lambda^3} + \mu_0 H(H + M_s) V \cdot R_a. \tag{37}$$

According to the results in Eq. (24), the total energy in hexagon spikes distribution pattern and square spikes distribution pattern can be obtained. (The density ρ of ferrofluids in this work is 1.346 g/cm^3. The surface tension σ of ferrofluids is 30.6 mN/m. The acceleration of gravity g is 9.8 m/s^2. Saturated magnetization M_s of ferrofluids is 24.5 emu/g). As shown in Fig. 9(a), the results of the total energy of a single spike E_{tot} in Rosensweig instability *versus* magnetic field H in perturbation of magnetic field are obtained. Considering the perturbation field results, the total energy of hexagonal pattern is greater than that in square pattern. It is indicated that the energy used to construct spikes in hexagonal pattern is larger than constructive energy in square pattern. The part of contribution of repulsive potential is about 1 orders of magnitude smaller constructive energy of spikes. The hexagonal pattern has a denser packed-form of distribution than the square pattern, which ensures the hexagonal pattern become the final pattern with spikes' distribution under small perturbation field intensity.

In contrast, the Rosensweig instability with large magnetic field has a different control equation in Eq. (31). The wavelength λ and amplitude A could be largely affected by

the strength of external magnetic field. The calculation results of the total energy E_{tot} are summarized by Eq. (37). As depicted in Fig. 9(b), the spikes patterns of Rosensweig instability under large magnetic field intensity are more complex than that under small perturbation field intensity. It has the same hexagonal patterns under compared weak magnetic field. As the magnetic field intensity H raises, the magnetic repulsive potential E_r gradually becomes the main contribution to total energy of a single spike E_{tot}. There is a cross point between the total energy of a single spike E_{tot} of hexagonal patterns and square patterns, namely, hexagon–square transition point. When the field intensity H is larger than that of the transition point H_t, the spikes of Rosensweig instability exhibit standard square patterns. This is perfectly corresponded with the experimental results.

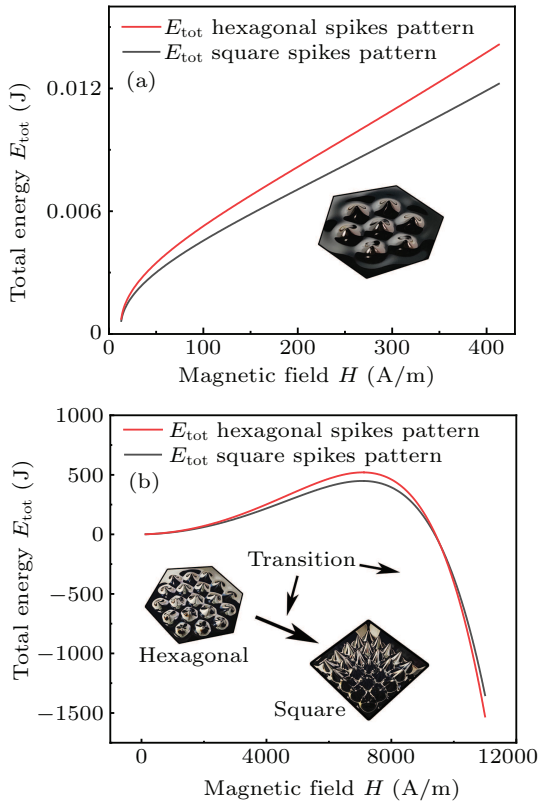


Fig. 9. (a) Total energy of a single spike E_{tot} in Rosensweig instability *versus* magnetic field H in perturbation of magnetic field, (b) total energy of a single spike E_{tot} in Rosensweig instability *versus* magnetic field H with large magnetic field strength.

3. Conclusions

Rosensweig instability is a kind of mysterious phenomenon that has been discussed for many decades. In this study, the control equations of Rosensweig instability spikes are systematically discussed. Based on the NS equation, a standard elliptical equation of Rosensweig instability spikes is constructed, providing a conclusion that the spikes of Rosensweig instability have some nature of wave property, which is corresponded with the experimental results that the spikes' pattern can detect the container wall and spread evenly in the container. It is difficult to solve this NS equation directly. Inspired by the linear stability analysis theory proposed by Rosensweig, the magnetic field intensity could be divided into 2 parts. The perturbation part NS equation that has been solved gets a similar conclusion (cosine wave solution in Eq. (24) of the linear stability analysis theory raised by Rosensweig. However, the perturbation results are only suited for field intensity H close to critical intensity H_c ($\sim$ 13 A/m). Herein, this study has established a large field hypothesis to solve the other part that cannot be easily solved by perturbation model. Based on such a model, a final hyperbolic tangent form of solution of wave Rosensweig instability spikes is obtained, which is presented as Eq. (31). For the purpose of evaluating the accuracy of the equation, this study compares the results of experimental results of central spike and side spikes and theoretical results predicted by the hyperbolic tangent form of solution in Figs. 6 and 7. The theoretical results are well fitted to the experimental results, which indicates that the spikes of Rosensweig instability have a hyperbolic tangent form when the magnetic field is greatly larger than the critical strength H_c. By introducing the hyperbolic tangent form model, this study successfully explaines the nature of hexagon–square transition of spikes theoretically. When the magnetic field intensity is less than the field intensity of transition point, the high efficiency of hexagonal close packing of spikes brings higher energy to construct the spikes with same field intensity H compared with the square pattern of spikes distribution. As the field intensity H increases to larger than transition field intensity H_t, the repelling potential E_r become the main obstacle for spikes' pattern construction in Rosensweig instability. The hexagon–square transition is successfully explained through these theoretically results. This theoretical model results could be further adopted to explain other phenomenon of Rosensweig instability in future.

Acknowledgements

Project supported by the National Natural Science Foundation of China (Grant Nos. 51735006, 51927810, and U1837206) and Beijing Municipal Natural Science Foundation (Grant No. 3182013).

References

[1] Cowley M D and Rosensweig R E 1967 *J. Fluid Mech.* **30** 671
[2] Gailitis A 1977 *J. Fluid Mech.* **82** 401
[3] Cao Y and Ding Z J 2014 *J. Magn. Magn. Mater.* **355** 93
[4] Rosensweig R E 1987 *Annu. Rev. Fluid Mech.* **19** 437
[5] Gollwitzer C, Rehberg I and Richter R 2006 *J. Phys.: Condes. Matter* **18** S2643
[6] Abou B, Wesfreid J E and Roux S 2000 *J. Fluid Mech.* **416** 217
[7] Kubstrup C, Herrero H and PerezGarcia C 1996 *Phys. Rev. E* **54** 1560
[8] Gollwitzer C, Matthies G, Richter R, Rehberg I and Tobiska L 2007 *J. Fluid Mech.* **571** 455

[9] Matthies G and Tobiska L 2005 *J. Magn. Magn. Mater.* **289** 346
[10] Li L, Li D C and Zhang Z L 2022 *Front. Mater.* **10** 893072
[11] Li L, Li D C and Zhang Z L 2022 *J. Magn. Magn. Mater.* **564** 170096
[12] Li L, Li D C, Wang L, Liang Z Q and Zhang Z L 2023 *J. Magn. Magn. Mater.* **12** 171077
[13] Tita A and Vanichchapongjaroen P 2018 *Mod. Phys. Lett. A* **16** 1850195
[14] Engel A, Lange A, Langer H, Mahr T and Chetverikov M V 1999 *J. Magn. Magn. Mater.* **201** 310
[15] Lange A, Langer H and Engel A 2000 *Physica D* **140** 294
[16] Rosensweig R E 1966 *Nature* **210** 613
[17] Kats E I 2011 *Low Temp. Phys.* **37** 812
[18] Spyropoulos A N, Papathanasiou A G and Boudouvis A G 2019 *J. Fluid Mech.* **870** 389
[19] Shaked H 1974 *Phys. Lett. A* **50** 385
[20] Dormann J L, Bessais L and Fiorani D 1988 *J. Phys. C-Solid State Physics* **21** 2015
[21] Panczyk T, Warzocha T P and Camp P J 2010 *J. Phys. Chem. C* **114** 21299
[22] Hoppe R 1966 *Angew. Chem. Int. Edit.* **5** 95
[23] Friedrichs R and Engel A 2001 *Phys. Rev. E* **10** 021406